Mesoporous Materials

DOI: 10.1002/ange.200605048

Mesostructured Manganese Oxide/Gold Nanoparticle Composites for Extensive Air Purification**

Anil K. Sinha, Kenichirou Suzuki, Minoru Takahara, Hirozumi Azuma, Takamasa Nonaka, and Kazuhiro Fukumoto*

Strong public concern and increasingly strict legislations[1] have made it highly imperative to devise versatile materials that can efficiently eliminate a wide range of organic pollutants from indoor and outdoor emissions. These pollutants contribute to photochemical smog and ground-level ozone and have raised severe concern owing to probable short- and long-term adverse health effects.[2] Most air-purification systems are based on photocatalysts, adsorbents such as activated carbon, or ozone-promoted oxidation.[3] However, all the currently used materials have limited efficiency in removing several volatile organic compounds (VOCs) under ambient conditions. Herein, we report a novel mesoporous manganese oxide/nanogold catalyst for efficient elimination of VOCs. To the best of our knowledge, γ-MnO_2 materials reported to date have surface areas of no higher than 130 $m^2 g^{-1}$.[4] In the present study, mesoporous γ-MnO_2 with a very high surface area (>300 $m^2 g^{-1}$) was obtained for the first time through a surfactant-assisted wet-chemistry route. Au nanoparticles were deposited on this oxide by a vacuum ultraviolet radiation (VUV)-assisted laser ablation (VALA) method to induce lattice defects[5,6] and strong metal–support interactions.[7] The material reveals an exceptionally good ability to remove VOCs (as well as NO_x and SO_2) at ambient temperature, and this efficiency increases with increasing temperature. The high activity of these materials could be correlated to their redox properties and to the facile formation of radical species on their surface.

We recently reported that high-surface-area mesoporous metal oxide materials are capable of eliminating VOCs at ambient temperature.[8–12] With these promising results in hand, we investigated a range of metal oxides and noble-metal catalysts and found that mesoporous γ-MnO_2 with a very high surface area and modified with gold nanoparticles can efficiently eliminate a wide range of VOCs under ambient dark conditions. We chose three different classes of VOCs, namely acetaldehyde, toluene, and *n*-hexane, which are major components of indoor as well as outdoor organic pollutants, to demonstrate the efficacy of our mesoporous γ-MnO_2/nanogold catalysts.

The mesoporous γ-MnO_2 material rapidly eliminated acetaldehyde, with complete removal achieved within 1 h at room temperature (Figure 1b; see also Figure S1 in the Supporting Information) and with 18% CO_2 formation after 24 h reaction (Figure 1a). The formation of CO_2 increased rapidly with a slight increase in the temperature and reached 94% at 60 °C (Figure 1a). This result indicates that the acetaldehyde is rapidly adsorbed onto the mesoporous γ-MnO_2 and gradually decomposes on its surface. The efficiency of acetaldehyde removal is about 2–3-times better than those of conventional materials used to remove VOCs (Figure 1b).

We studied acetaldehyde removal at different concentrations to evaluate the efficacy of these materials in comparison with traditional amelioration methods, such as using activated carbon, at very low "real-world" concentrations of VOCs (Figure 1c). Activated carbon revealed a rapid decrease in removal capacity with decreasing acetaldehyde concentrations, but interestingly the mesoporous γ-MnO_2 exhibited only a very gradual decrease. The removal capacity of acetaldehyde nearly doubled after Au deposition on the mesoporous material. At acetaldehyde concentrations as low as 2 ppm, mesoporous γ-MnO_2 revealed a removal capacity that was about 25-times higher than that of activated carbon while the removal capacity of Au-deposited mesoporous γ-MnO_2 was around 50-times higher.

Mesoporous γ-MnO_2 showed approximately 60% toluene removal at 25 °C (which increased to about 93% at 85 °C) but less than 2% hexane removal even at 85 °C (Figure 1d) from a mixture of toluene, acetaldehyde, and *n*-hexane. However, after Au deposition (2.8 wt%, particle size 3–6 nm) on mesoporous γ-MnO_2, the elimination of VOCs was dramatically enhanced; the γ-MnO_2/Au material revealed about 95% toluene removal and 30% *n*-hexane removal at 25 °C (Figure 1d), that is, enhancement of nearly 1.6-fold and 15-fold, respectively, after Au deposition. The removal efficiency was further enhanced by increasing the reaction temperature to 85 °C, with 99% toluene removal and 77% *n*-hexane removal (Figure 1d; see also Figure S2 in the Supporting Information). Adsorbed VOCs could be decomposed below 250 °C, and the regenerated catalyst could be reused. Moreover, the Au particles did not show any significant agglomeration at higher temperatures, as a result of strong metal–support interactions.

In the case of toluene removal, the mesoporous γ-MnO_2 sample revealed 5% CO_2 formation at 25 °C (after 24 h) which increased to 55% at 85 °C (Figure S3 in the Supporting Information). In a flow reactor, approximately 40% toluene

[*] Dr. A. K. Sinha, K. Suzuki, M. Takahara, H. Azuma, T. Nonaka, K. Fukumoto
Toyota Central R&D Labs Inc.
41-1, Aza, Yokomichi, Nagakute-cho
Aichi-gun, Aichi-ken 480-1192 (Japan)
Fax: (+81) 561-63-6137
E-mail: sinha-anil@mosk.tytlabs.co.jp

[**] We thank N. Suzuki and N. Takahashi of Toyota CRDL Inc. for TEM and XPS analyses, respectively.

Supporting information for this article is available on the WWW under http://www.angewandte.org or from the author.

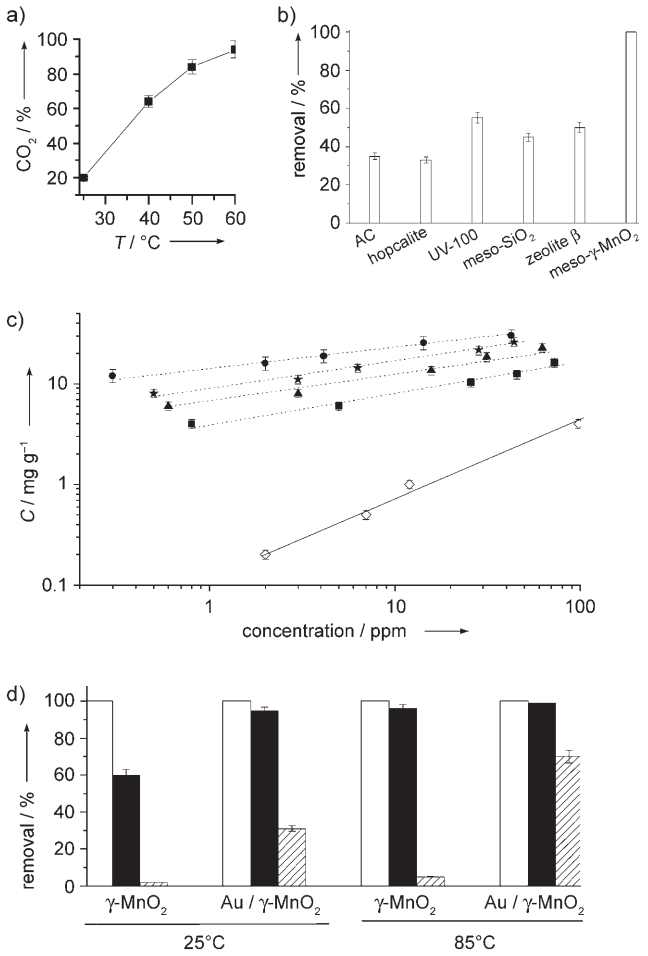

Figure 1. The efficiency of removal of VOCs from air. a) Formation of CO_2 over mesoporous γ-MnO_2 during the removal of acetaldehyde (24 h). b) Efficiency of the mesoporous γ-MnO_2 sample (meso-γ-MnO_2) in removing acetaldehyde in comparison with that of conventionally used materials (1 h, 100 mg samples): activated carbon (AC), hopcalite, titania (UV-100, under UV irradiation using 500-W high-pressure mercury arc lamp), mesoporous silica (meso-SiO_2), and microporous zeolite beta. c) Comparison of the acetaldehyde removal capacities *C* [mg(acetaldehyde) per g(substrate)] of mesoporous γ-MnO_2 and Au-deposited mesoporous γ-MnO_2 in comparison with conventionally used activated carbon (1060 $m^2 g^{-1}$). Activated carbon (◇), γ-MnO_2 (25 °C; ■), γ-MnO_2 (40 °C; ▲), Au/γ-MnO_2 (25 °C; ⋆), Au/γ-MnO_2 (40 °C; ●). d) Efficiencies of mesoporous γ-MnO_2 and Au-deposited mesoporous γ-MnO_2 in removing toluene (filled), acetaldehyde (empty), and hexane (hatched) following exposure for 24 h.

decomposition was achieved well below 100 °C and it was possible to reach 100 % toluene combustion at about 220 °C and 250 °C for Au-loaded and Au-free catalysts, respectively (Figure S4 in the Supporting Information). Relative to the best performing material, namely mesoporous chromium oxide,[8,9] the mesoporous manganese oxide here shows 3–5-times higher conversion of CO_2 under similar reaction conditions. Mesoporous Mn_2O_3, nonporous commercial MnO_2, and hopcalite materials showed less than 10 % toluene removal (Figure S3 in the Supporting Information) without any CO_2 formation. We also found that mesoporous γ-MnO_2 displays a good performance in the removal of NO_x (72 mg g^{-1}) and SO_2 (700 mg g^{-1}; see Supporting Information).

Several factors are responsible for the good ability of mesoporous γ-MnO_2 to remove VOCs (as well as NO_x and SO_2): 1) A hierarchical structure resulting from aggregates of near-spherical microparticles of approximately 1 μm in size (from scanning electron microscopy, Figure S5 in the Supporting Information) which result from the physical packing of nanometer-sized fibrous particles (from transmission electron microscopy (TEM), Figure 2a). Furthermore, the

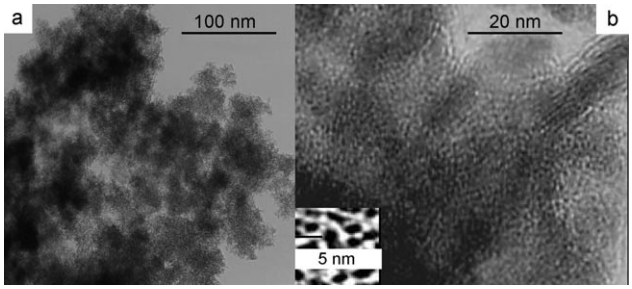

Figure 2. TEM images of mesoporous manganese oxides show a) nanofibrous aggregates and b) the disordered wormholelike mesoporosity.

fibrous particles consist of intraparticle disordered mesoporosity (from TEM, Figure 2b). Such a structure would furnish a large number of adsorption sites. 2) Possible structural distortions resulting from a mesoporous nanocrystalline structure (wide-angle X-ray diffraction (XRD) shows very weak and broad peaks for γ-MnO_2, Figure S6 in the Supporting Information) as well as γ-MnO_2 being an intergrowth structure (made up of ramsdellite randomly interspersed with pyrolusite) could result in a large number of point defects and vacancies. 3) The mesoporous γ-MnO_2 in the present study has a very high surface area of 316 $m^2 g^{-1}$ (mean pore size 3.6 nm, Figure S7 in the Supporting Information), which is the highest surface area reported for manganese oxide (about 2.4-times higher than the highest previously reported[4]). This feature would result in a high sorption capacity and a large number of active sites. 4) Readily available lattice oxygen for oxidation (see below).

Manganese oxide/gold catalysts prepared by a co-precipitation method have been reported to be active catalysts for low-temperature CO oxidation reactions.[13] In the present study, deposition of gold nanoparticles on mesoporous γ-MnO_2 by the classical deposition–precipitation method[14] resulted in a catalyst with poor activity (XRD showed the formation of a mixed manganese oxide phase after Au deposition, while TEM showed Au agglomerates of over 25 nm in size). Attempts to use the low-energy (200 MW cm^{-2}) laser-ablation process to deposit metal nanoparticles resulted in very little improvement in the performance of the catalyst in the removal of VOCs. However, surprisingly, a dramatic enhancement in the ability of the substrate to remove VOCs was observed after the deposition of Au by the VALA method. The VALA method[15] produces laser plasma containing highly energetic ablated Au nano-

particles that deposit on the mesoporous substrate. VUV photons produced during this process (in the wavelength region 60–80 nm) can induce both thermal activation and lattice defects.[5,6] γ-MnO_2 shows a strong absorption at $\lambda \approx 60$ nm in the VUV region (see Figure S8 in the Supporting Information) which can be expected to result in rapid activation of this material during Au deposition by the VALA method. Au nanoparticles of 3–6 nm in size were well dispersed (Figure 3a) and clearly seen to be embedded in the

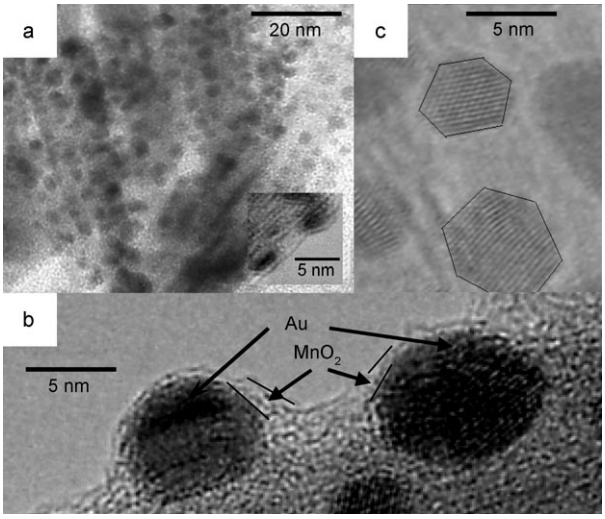

Figure 3. a) TEM image of 3–10-nm Au nanoparticles on the mesoporous γ-MnO_2 surface (the inset shows Au nanoparticles in the mesopore). b) High-magnification transmission electron micrograph showing Au nanoparticles embedded in the γ-MnO_2 lattice to create a unique interface. c) HRTEM image shows the formation of well-facetted Au nanoparticles.

support lattice (Figure 3b), as a result of the high-energy Au deposition method as well as the easily penetrable structure of the mesoporous support. Some Au nanoparticles were observed inside mesoporous channels (Figure 3a, inset). These observations indicate very strong metal–support interactions[7] after Au deposition, which creates a unique interface that results in enhanced activity. High-resolution (HR)-TEM revealed that the Au nanoparticles are well facetted (Figure 3c).

Au L3-edge X-ray absorption near-edge structure (XANES) analysis confirmed that Au nanoparticles are completely metallic. However, X-ray photoelectron spectroscopy (XPS) analysis revealed Au^0 binding energies at 84.6 and 88.2 eV, which are 0.6 eV higher than those for bulk metallic Au (84.0 and 87.6 eV). This small shift in binding energy indicates a partial positive charge ($\delta+$) on Au sites resulting from strong electronic interaction between the metal and the support. The binding energy for the Mn species is the same for Au-loaded and Au-free samples (642.5 eV) which corresponds to a +4 oxidation state for Mn. XPS analysis did not reveal any change in the oxidation states (binding energies) of Au and Mn following their reaction to remove VOCs. However, Mn K-edge XANES spectra of a sample of Au-deposited mesoporous γ-MnO_2 after exposure to toluene (100 ppm in air, 24 h) revealed that the oxidation state of Mn decreases slightly (reduction, ≈1.1 eV edge shift, Figure 4) and that this decrease in oxidation state is greater at higher temperatures (≈2.6 eV edge shift, Figure 4). Interestingly,

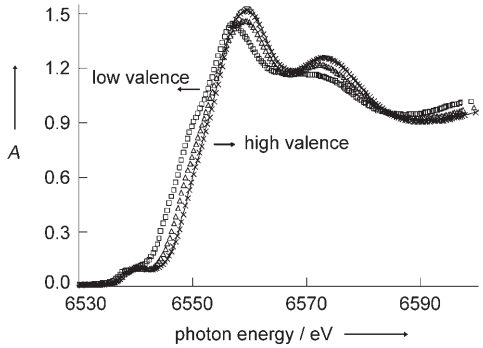

Figure 4. Mn K-edge XANES spectra of Au-deposited mesoporous γ-MnO_2: a fresh sample (——) was reduced by toluene at 85 °C (△) and at 200 °C (○). The reduced sample was reoxidized in air at 100 °C (×). The material can readily undergo partial reduction–oxidation cycles under reducing and oxidizing conditions.

the material easily readopted its original oxidation state after heating the reduced sample in air at 100 °C (Figure 4). These observations clearly show that the MnO_2 lattice oxygen atoms are readily available for oxidation and are involved in the oxidation of the VOCs, in accordance with the Mars–van Krevelen mechanism.[16] A two-step Mars–van Krevelen model involving an exchange between the gas phase and lattice oxygen has also been proposed for the oxidation of benzyl alcohol by molecular O_2 in the liquid phase using an octahedral molecular sieve (OMS) catalyst.[17] Analysis of local structure parameters around Mn shows that the coordination number of Mn (Table 1 in the Supporting Information) is lowered after Au deposition, possibly as a result of strong metal–support interactions. The coordination number also decreased after exposure of the sample to toluene, and this decrease is greater at higher temperatures, thus indicating a strong interaction between the adsorbed toluene and the oxide lattice.

It is also likely that oxygen can dissociate on the Au surface and spill over from Au to the oxygen vacancies in the oxide, which synergetically promotes the adsorption/dissociation of VOCs. In situ ESR analysis of Au/MnO_2 samples after evacuation and exposure to oxygen showed a weak anisotropic signal which can be attributed to the formation of radical species on the surface of this catalyst (see Figure S9 in the Supporting Information). The ability to form such radical species in the presence of oxygen[18] is probably the reason for the enhanced performance of the Au-deposited material in removing VOCs.

In summary, these findings clearly show the efficacy of high-surface-area mesoporous γ-MnO_2 materials in the removal of VOCs. Moreover, the efficiency is dramatically enhanced after deposition of gold nanoparticles on the substrate by a VALA process. These materials also have excellent potential for applications in energy devices, oxidation catalysts, catalyst supports, and adsorbents. The novel

process for the deposition of nanogold on a substrate should also be suitable for the preparation of efficient catalysts for several other applications.

Experimental Section

A precipitate formed by mixing an aqueous solution (0.06 M, 100 mL) of $Mn(NO_3)_2{\cdot}6H_2O$ with a solution of NaOH (0.12 M, 25 mL) was added to an aqueous solution of cetyltrimethylammonium bromide (60 g in 150 mL water) at pH 8.0. The resulting gel (pH 10.5) was heated for 20 h at 75 °C in a closed vessel. The solid residue was filtered, washed with water, dried in air, and finally calcined at 500 °C for 4 h (1° min^{-1}.). The calcined sample (6.0 g) was stirred in 10 M aqueous H_2SO_4 solution (300 mL) for 30 min, filtered, washed with water, and dried at 105 °C to obtain mesoporous γ-MnO_2 sheets.

The second harmonic of a Nd:YAG pulsed laser (4.8 GW cm^{-2})[11] with a pulse width of 7 ns and energy of 1 J $pulse^{-1}$ was used to vaporize the Au metal from an Au disk to create a plasma. The supports, prepared as thin sheets, were placed in front of the cluster beam. Each side of the wafer was exposed to the cluster beam for the same time interval (15 min). The metal content was measured by chemical analysis (inductively coupled plasma).

For the analyses, a gas mixture (5 L) was used which contained VOCs (103.3 ppm toluene or 200 ppm acetaldehyde or a mixture of 19.5 ppm toluene and 27 ppm acetaldehyde and 50 ppm hexane), 20% oxygen, and the balance of nitrogen. The samples of MnO_2 (0.3 g) and the gas were introduced in a 5-liter container. The gas was analyzed by GC (Shimadzu GC-12A) and a CO_2 analyzer (LI-COR, Inc.). The percentage removal of VOCs was calculated from the concentration of gas in the container according to Equation (1), while

$$\%\,\text{removal} = \left(1 - \frac{\text{concentration of gas with catalyst}}{\text{concentration of gas without catalyst}}\right) \times 100 \quad (1)$$

the conversion of VOCs was calculated on the basis of the CO_2 formed.

Received: December 14, 2006
Published online: March 6, 2007

Keywords: adsorption · gold · manganese · mesoporous materials · oxidation

[1] US Environment Protection Agency: Clean Air Act, (**1993**; http://www.epa.gov/iaq/voc.html).
[2] H. K. Hudnell, D. A. Otto, D. E. House, L. Molhave, *Arch. Environ. Health* **1992**, *47*, 31.
[3] K. Yogo, M. Ishikawa, *Catal. Surv. Jpn.* **2000**, *4*, 83.
[4] J. Yuan, K. Laubernds, Q. Zhang, S. L. Suib, *J. Am. Chem. Soc.* **2003**, *125*, 4966.
[5] N. Kristianpoller, D. Weiss, R. Chen, *Phys. Status Solidi C* **2005**, *2*, 409.
[6] A. Stesmans, V. V. Afanas'ev, *Appl. Phys. Lett.* **2000**, *77*, 1469.
[7] C. M. Y. Yeung, K. M. K. Yu, Q. J. Fu, D. Thompsett, M. I. Petch, S. C. Tsang, *J. Am. Chem. Soc.* **2005**, *127*, 18010.
[8] A. K. Sinha, K. Suzuki, *Angew. Chem.* **2005**, *117*, 275; *Angew. Chem. Int. Ed.* **2005**, *44*, 271.
[9] A. K. Sinha, K. Suzuki, *Appl. Catal., B* **2007**, *70*, 417.
[10] A. K. Sinha, K. Suzuki, *J. Phys. Chem. B* **2005**, *109*, 1708.
[11] A. K. Sinha, K. Suzuki, *Int. J. Appl. Ceram. Technol.* **2005**, *2*, 476.
[12] "Clean Air" (research highlight), *Nat. Mater.* **2005**, *4*, 187.
[13] S.-J. Lee, A. Gavriilidis, Q. A. Pankhurst, A. Kyek, F. E. Wagner, P. C. L. Wong, K. L. Yeung, *J. Catal.* **2001**, *200*, 298.
[14] A. K. Sinha, S. Seelan, S. Tsubota, M. Haruta, *Angew. Chem.* **2004**, *116*, 1572; *Angew. Chem. Int. Ed.* **2004**, *43*, 1546.
[15] H. Azuma, A. Takeuchi, N. Kamiya, T. Ito, M. Kato, S. Shirai, T. Narita, K. Fukumori, K. Tachi, T. Matsuoka, *Jpn. J. Appl. Phys.* **2004**, *43*, L1250.
[16] P. Mars, D. W. van Krevelen, *Chem. Eng. Sci.* **1954**, *3*, 41.
[17] a) Y.-C. Son, V. D. Makwana, A. R. Howell, S. L. Suib, *Angew. Chem.* **2001**, *113*, 4410; *Angew. Chem. Int. Ed.* **2001**, *40*, 4280; b) V. D. Makwana, Y.-C. Son, A. R. Howell, S. L. Suib, *J. Catal.* **2002**, *210*, 46.
[18] A.-Q. Wang, C.-M. Chang, C.-Y. Mou, *J. Phys. Chem. B* **2005**, *109*, 18860.

